

Uncertainty of the Measurement of Radial Runout, Axial Runout and Coning using an Industrial Axi-Symmetric Measurement Machine

J E Muelaner, A Francis, P G Maropoulos

The Laboratory for Integrated Metrology Applications, Department of Mechanical Engineering, The University of Bath, Bath, UK

Abstract. This paper describes an uncertainty evaluation for the measurement of radial runout, axial runout and coning for axi-symmetric measurement machine. An industrial axi-symmetric measurement machine was used which consisted of a rotary table and a number of contact measurement probes located on slideways. Type A uncertainties were obtained from a repeatability study of the probe calibration process, a repeatability study of the actual measurement process, a system stability test and an elastic deformation test. Type B uncertainties were obtained from calibration certificates and estimates. Expanded uncertainties, at 95% confidence, were then calculated for the measurement of; radial runout (1.2 μm with a plunger probe or 1.7 μm with a lever probe); axial runout (1.2 μm with a plunger probe or 1.5 μm with a lever probe); and coning/swash (0.44 arc seconds with a plunger probe or 0.60 arc seconds with a lever probe).

Keywords: Axial Runout, Radial Runout, Coning, Uncertainty of Measurement, Light Controlled Factory

3924.1 Introduction

Measurements of axial runout, radial runout and coning are important for axi-symmetric components and are of increasing interest for the optimisation of tolerances within measurement assisted manufacturing systems [1]. For example when assembling compressor stages within gas turbine engines accurate measurements of each component allow the assembly sequence and orientation to be optimized to minimize deviations in the assembly.

An axi-symmetric measurement machine, **Fig. 1**, is a specialized measuring machine for the inspection of axisymmetric components enabling the measurement of properties such as roundness (radial runout), axial runout and coning. It consists of a rotary table and a number of contact measurement probes located on slideways. The probes allow small deviations in the part to be measured as it is rotated and the slideways allow the probes to be manually positioned at different locations on the component. Such machines form an

integral part of the emerging Light Controlled Factory manufacturing paradigm [2].

This paper describes an uncertainty evaluation for the calibration uncertainty of an industrial axi-symmetric measurement machine; the iMAP machine from RPI.



Fig. 1 – An Axi-Symmetric Measurement Machine

The rapidly developing Geometric Product Specification (GPS) standards [3] fully embrace the concept of uncertainty of measurement stating that measurements should always be accompanied by a quantitative indication of uncertainty [4, 5] which establishes a range of values within which there is confidence that the true value lies. This means that all factors affecting the measurement result must be considered, not simply repeatability and reproducibility. In addition to repeatability (random variation under constant conditions) and reproducibility (differences in results under different conditions such as different operators) sources such as the uncertainty of the reference standard, environmental factors such as temperature, alignments and setup parameters, and rounding errors should all be considered. Quantified uncertainties for each factor

may be classed as Type A (obtained by statistical analysis of a series of observations) or Type B (obtained by other means). All uncertainties are then modelled as probability distributions and quantified as variances which are statistically combined to give a combined standard uncertainty [4, 5]. Finally the standard uncertainty is expanded by a coverage factor to give bounds to the possible range of values within which the true value may lie, at a given confidence level.

According to the Procedure for Uncertainty Management (PUMA) components of uncertainty may be initially given approximate ‘worst case’ estimates to enable a combined uncertainty to be calculated. It is then possible to determine which sources are significant and obtain improved estimates for these sources. This process can be repeated until a satisfactory estimate of uncertainty is obtained [6].

3924.2 Sources of Uncertainty for Axi-Symmetric Measurement

The sources of uncertainty in the measurements of radial runout, axial runout and coning can be classified under six categories; Probe Calibration using gauge calibrator; use of probe; alignment of probe to part; rotary table geometric errors; dimensional stability of structure; and reference hemisphere. Each of these is described in the sub-sections below.

3924.2.1 Probe Calibration

Before use on the measurement machine the probe is separately calibrated using a micrometer based gage calibrator. On the measurement machine the probe makes measurements of the relative displacement of the artefact as it is rotated, therefore it is not necessary to establish a zero point accurately. As the probe is moved through a series of discrete displacements its voltage output is recorded along with the reference displacement as measured by the gage calibrator. These measurements are used to characterise the probe. For a plunger type probe this characterisation takes the form of a single sensitivity value while for a lever probe a 5th order polynomial is used to model the relationship between displacement and voltage output.

Sources of uncertainty in the probe calibration are; the uncertainty of the gage calibrator; the repeatability of the calibration process; the fitting error; and the probe resolution. The calibrator uncertainty is taken from the calibrator’s calibration certificate and includes the uncertainty accumulated along the traceability chain. The probe calibration repeatability is the random variation between different calibrations;

this includes process repeatability such as probe alignment, human error, differences in torque applied with tightening the screw and other differences between different operators.

3924.2.2 Use of Probe

When the probe is actually measuring displacements as a components is rotated in the measurement machine uncertainties are encountered due to; the probe resolution; probe reversal spikes; and probe repeatability. Probe resolution is the resolution of the voltage reading from the probe and results in an uncertainty which is half of the smallest increment. The probe reversal spike is a dynamic error which occurs when the probe's moving stylus tip changes its direction of motion. Probe repeatability is lumped into a system repeatability study which includes all sources of repeatability for the measurement machine.

3924.2.3 Alignment of Probe to Part

Uncertainty in the alignment of the probe to the part results in an uncertainty in the result of the measurement; angular offset between the probe’s axis of measurement and the nominal surface normal results in *cosine error*; and offset between the probe's point of contact and the true center line of the circular artefact results in *off-centre error*.

When the probe is aligned normal to the surface of the part there is no cosine error since a change in the part radius dr will result in an equal movement of the probe dM . When there is an angular offset between the probe’s axis of measurement and the nominal surface normal, this will result in a cosine error so that dM is no longer equal to dr as shown in **Fig. 2**. The cosine error E_c is the difference between the actual change in radius and the measured distance.

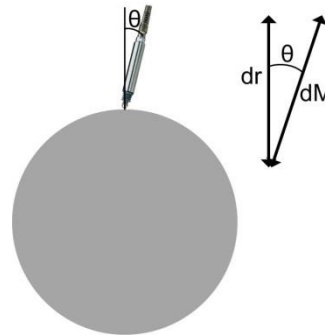


Fig. 2 – Probe Cosine Error

$$\cos \theta = \frac{dr}{dM} \quad (1)$$

$$E_c = \frac{dr}{\cos \theta} - dr \quad (2)$$

When there is an offset dy between the probe's point of contact and the true center line of the circular artefact, this results in off-centre error. When the radius changes by dr the probe will measure a change of dM .

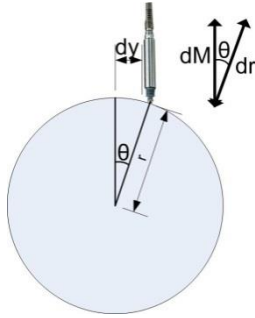


Fig. 3 – Probe Off-Centre Error

$$dM = dr \cdot \cos \theta \quad (3)$$

The probe off-centre error is the difference between the actual change in radius dr and the measurement result dM .

$$E_c = dr(1 - \cos \theta) \quad (4)$$

The angle θ is a function of the radius and the offset dy

$$\theta = \arcsin\left(\frac{dy}{r}\right) \quad (5)$$

So the probe off-centre error can be stated as

$$E_c = dr \left(1 - \cos \left(\arcsin \left(\frac{dy}{r} \right) \right) \right) \quad (6)$$

3924.2.4 Table geometric errors

Geometric errors such as swash, radial runout and axial runout occur in the movement of the rotary table within the measurement machine. These cause errors in measurement. There is also an interaction between the measurement of radial and axial runout due to a hemisphere being used in the calibration process.

Swash is the result of the axis of symmetry for the axi-symmetric component not being aligned to the axis of rotation for the rotary table of the machine. This

causes an apparent eccentricity when the part is rotated which increases linearly with distance along the axis.

Axial and radial runout are the vertical and radial movements of the table as it is rotated due, these occur due to imperfections in the table's mechanism

The interaction between the measurements of axial and radial runout occurs because a hemisphere is used. For example, when measuring axial runout the probe is placed at the top of the hemisphere to measure any vertical movement. Radial runout will cause the hemisphere to move sideways and since the top surface is not flat this will result in an apparent vertical movement when monitoring the probe reading as illustrated in Fig. 4.

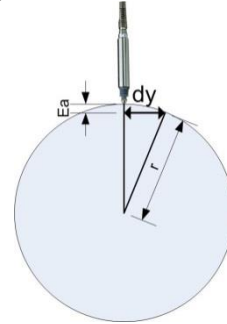


Fig. 4 – Axial/Radial Runout Interaction

Considering a horizontal movement of the reference hemisphere due to radial runout dy , the resulting displacement of the probe E_a and the hemisphere radius r forming a right angle triangle we can say that

$$dy^2 + (r - E_a)^2 = r^2 \quad (7)$$

Rearranging this gives the error due to radial interaction on axial runout E_a

$$E_a = r - \sqrt{r^2 - dy^2} \quad (8)$$

The axial interaction of radial runout and the radial interaction on axial runout are equal and can be shown to be negligible.

3924.2.5 Dimensional Stability of Structure

Thermal expansion of the structure, vibration and elastic deformation under dynamic loadings may cause errors in measurement. The uncertainty due to these sources can be evaluated by monitoring probe deflection over a period of time equivalent to a typical measurement and during which maximum thermal variation is encountered, such as opening a door or exposing the instrument to direct sunlight.

3924.2.6 Reference Hemisphere

Imperfections in the reference hemisphere used for calibration will induce errors. The uncertainty in the Hemisphere’s roundness, taken from it’s calibration certificate, therefore contributes to the uncertainty of the measurement machine. The position of the hemisphere on the rotary table will also produce apparent errors in the measurement of radial runout and, although these are corrected for using a best-fitting algorithm, residual errors will remain.

3924.3 Procedure used for Uncertainty Evaluation

The uncertainty evaluation procedure used enables the effects of all of the above sources of uncertainty to be quantified. This follows the sequence shown in Fig. 5 with the values obtained at each stage being used to calculate the combined uncertainty using an uncertainty budget with sensitivity coefficients derived from the equations above.

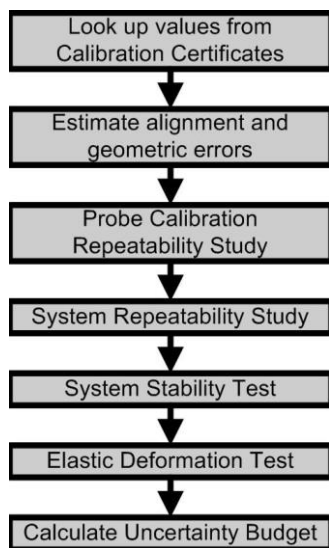


Fig. 5 – Uncertainty Evaluation Process

3924.3.1 Step 1: Look Up Values for Type B Uncertainties and Critical Dimensions

First Type B uncertainties were obtained from calibration certificates and specified dimensions for; the probe calibrator’s calibration uncertainty; the probe rounding error; the probe calibrator rounding error; the reference hemisphere roundness; the reference hemisphere radius; and the reference hemisphere calibration uncertainty. The values for these are shown in Table 1.

Table 1 – Values Recorded in Step 1

Source	Value
Probe Calibrator Instrument Uncertainty (k=1 value)	1 µm
Smallest Increment of probe reading (2x resolution uncertainty)	0.0001 V
Smallest Increment on probe calibrator (2x resolution uncertainty)	0.1 µm
Reference Hemisphere radius	25 mm
Reference Hemisphere component peak	0.004 µm
Reference Hemisphere component valley	-0.004 µm
Reference Hemisphere Calibration Uncertainty	0.006 µm

3924.3.2 Step 2: Estimate Alignment and Geometric Errors

Worst case estimates for alignment and geometric errors showed these to have a negligible effect on the combined uncertainty. It was therefore determined that, according to the PUMA method worst case estimates were sufficient and accurate evaluation of these uncertainties was not attempted.

Table 2 – Values Estimated in Step 2

Source	Value
Offset of probe from component centre-line	3 mm
Change in component radius	10 µm
Eccentricity	10 µm
Angular offset (cosine error) for plunger probe	5°
Angular offset (cosine error) for lever probe	15°
Perpendicular Movement (radial runout when measuring axial etc)	25 µm

These estimates were used to calculate; Off-Centre Error; Cosine Error for plunger probe; Cosine Error for lever probe; and Axial-Radial Runout Interaction using the above equations. The results are given in Table 3.

Table 3 – Calculated Alignment and Geometric Errors

Source	Value
Off-Centre Error	0.14452 µm
Cosine Error for plunger probe	0.0764 µm
Cosine Error for lever probe	0.70552 µm
Axial-Radial Runout Interaction	0.0125 µm

Although most of these are negligible the cosine error for the lever probe is significant uncertainty, in this case however the estimated angle relates to the operating procedure for the probe and can therefore be considered an accurate estimate.

3924.3.3 Step 3: Probe Calibration Repeatability Study

Variation in the calibration process and fitting errors when fitting a curve to the calibration data are sources of uncertainty. A repeatability study was carried out for each type of probe to determine both of these sources of uncertainty.

The calibration process involves moving the probe through a number of known displacements using the probe calibrator as a reference and recording the voltage output at each of these displacements. A curve is then fitted through the data points and the coefficients of this line are used to characterize the probe for subsequent measurement. For a plunger probe a simple straight line fit is used and therefore a single sensitivity coefficient characterizes the probe. For the lever probe the response is non-linear and a 5th Order polynomial is used.

In the repeatability study the calibration is carried out a number of times and the standard deviation in the gradient of the line at the zero point is calculated, this gives the repeatability of the probe calibration. The standard fitting error for the best fit line is also calculated for all trials giving the probe calibration fitting error. In this study 10 calibrations were carried out to determine the calibration repeatability.

The plunger probe was calibrated close to mid-region of the probe stylus travel where the voltage reading ranges from -1.500 V to +1.500 V giving a probe travel range of 0.60 mm. The effective range of the probe is 1 mm. The probe voltage of 0.000 was initially set as datum and then the probe is extended by 0.300 mm where the voltage (of close to -1.500 V) was recorded before commencing the probe calibration process. The probe was then compressed by 0.600 mm, using a Mitoyo calibrator, at a consistent step size of 0.010 mm giving 61 data points. A perfect plunger probe would give reading from -1.500 to 1.500 at an increment of 0.050 V. A straight line was fitted to the obtained data points using a least squares regression method in order to obtain the sensitivity of the probe in V/mm, it was therefore not necessary to carry out each calibration over exactly the same mid-range.

In order to reduce the time taken for the probe calibration repeatability study a number of different step sizes were evaluated. This indicated that there was a negligible difference in the calculated sensitivity and standard fitting error when the step size was increased

to 0.02 mm and therefore this increased step size was used for the repeatability study reducing the number of data points which were recorded to 31. Table 5 shows the calculated sensitivity and standard fitting error for each repetition. Based on these results the standard deviation in the sensitivity can be calculated to be 0.00112 V/mm. The mean standard error is 0.00074 V which is sufficiently small to show that any non-linearity in the probe has a negligible impact on overall uncertainty.

Table 5: Results of Plunger Probe Calibration Repeatability Study

Trial	Best fit Sensitivity (V/mm)	Standard Error In Gradient (V)
1	5.00471	0.00054
2	5.00247	0.00086
3	5.00174	0.00081
4	5.00191	0.00073
5	5.00397	0.00057
6	5.00171	0.00079
7	5.00300	0.00071
8	5.00272	0.00092
9	5.00232	0.00074
10	5.00453	0.00068

The lever probe has non-linear behaviour since the stylus rotates about a pivot point. As for the plunger probe the voltage reading was given in the range from -0.584 to +0.377 V.

Similar to the plunger probe calibration process, the probe voltage of 0.000 was initially set as datum and then the probe is displaced from -0.300 mm to +0.300 mm to record the voltage at every step point. Again calibrations were carried out at different step sizes to determine an optimum step size which in this case was found to be 0.050 mm. In this case there was a non-linear relationship between the probe displacement and the voltage output with a 5th order polynomial being fit using a least squares regression method. To enable a sensitivity coefficient to be calculated for use in the uncertainty budget this was linearized about the range +/-50 µm. Table 4 shows the calculated sensitivity for each repetition. Based on these results the standard deviation in the sensitivity can be calculated to be 2.58 mV/mm. The standard error in the fit of the 5th order polynomial was 0.15 mV.

Table 4: Results of Plunger Probe Calibration Repeatability Study

Trial	Best fit Sensitivity (V/mm)
1	1.040
2	1.045
3	1.045
4	1.045
5	1.040
6	1.040
7	1.040
8	1.040
9	1.040
10	1.045

3924.3.4 Step 4: System Repeatability Study

The radial runout, axial runout and coning were each measured 10 times using the calibrated hemisphere as a reference. The corresponding geometric errors of the table were given by the mean of these measurements while the standard deviation of the results gave the system repeatability.

The system repeatability includes the probe repeatability in use, structure vibration and probe reversal spikes. The value for the geometric error of the table also includes any residual hemisphere off-centering error and probe geometric errors.

Before carrying out the repeatability study the rotary table was setup for measurement using both the reference hemisphere and calibrated probes. When aligning the probes, the voltage reading was set to within 5 microns of zero. It doesn't have to be exactly zero because the interest lies in relative motion rather than absolute. The table was then run for two revolutions to allow it to stabilize.

For each of the ten repetitions in the repeatability study the following steps were carried out:

- 1) The plunger was positioned at the side and the lever at the top of the hemisphere (this is position A)
- 2) The radial runout (using plunger) and axial runout (using lever) were measured over for 10 revolutions.
- 3) The probe positions were reversed (this is position B)
- 4) The radial runout (using lever) and axial runout (using plunger) were measured over 10 revolutions.
- 5) The hemisphere was raised by a height of 520 mm (position C) using a stand.

- 6) The radial runout was measured over 10 revolutions using both probes. The coning/swash value is calculated.

Table 5 shows the results of the repeatability study.

Table 5 – Results of Repeatability Study

Probe	Measurement	Table Geometric Errors	System Repeatability
Plunger	Radial Runout	0.40 μm	0.16 μm
	Axial Runout	0.38 μm	0.14 μm
	Coning	0.15 arc sec	0.06 arc sec
Lever	Radial Runout	0.40 μm	0.37 μm
	Axial Runout	0.38 μm	0.12 μm
	Coning	0.15 arc sec	0.11 arc sec

3924.3.5 Step 5: System Stability Test

In order to determine the effects of thermal expansion on the machine structure, electrical creep in the probe reading and any other sources of drift due to environmental variation over the duration of the measurement process a system stability test was carried out. The probe was placed against the artefact and the output from the probe was recorded over 3 minutes which is the normal duration of a measurement.

While the test was being carried out various environmental disturbances were induced. A number of these tests were carried out with different types of environmental disturbance such as opening a door to introduce cold air to the measurement environment, exposing the machine to direct sunlight and operating other machinery to introduce vibration. The greatest of the ranges of observed values for these conditions was used in the overall uncertainty budget which was 0.001 V.

3924.4 Uncertainty Budget

Uncertainties budgets were created for radial runout using plunger and lever probes, for axial runout using plunger and lever probes, and for coning using plunger and lever probes. The uncertainty budget for radial runout using a plunger probe is (Table 6) is show as an example. Each took a similar form with some differences in the geometric errors and sensitivity coefficients used.

Table 6 – Uncertainty Budget for the Measurement of Radial Runout using a Plunger Probe

Source of Uncertainty	Absolute Value	Relative values	Distribution	Divisor	Sensitivity Coefficient	Absolute Standard Uncertainty (µm)	Relative Standard Uncertainty (µm/µm)
Calibrator Instrument Uncertainty	1 µm		Normal	2	1	0.500	
Probe calibration repeatability		0.00112 V/mm	Normal	1	0.2 mm/V		0.0002
Probe Calibration Fitting Error	0.000735 V		Rectangular	1.7321	200 µm/V	0.085	
Probe resolution (calibration)	0.00005 V		Rectangular	1.7321	200 µm/V	0.006	
Calibrator resolution	0.05 µm		Rectangular	1.7321	1	0.029	
Probe resolution (in use)	0.00005 V		Rectangular	1.7321	200 µm/V	0.006	
System repeatability	0.16 µm		Normal	1	1	0.162	
Table Radial Runout	0.40 µm		Rectangular	1.7321	1	0.228	
Probe cosine error	0.076 µm		Rectangular	1.7321	1	0.044	
Probe off-centre error	0.145 µm		Rectangular	1.7321	1	0.083	
Axial/Radial Runout Interaction	0.013 µm		Rectangular	1.7321	1	0.007	
System Stability	0.0005 V		Rectangular	1.7321	200 µm/V	0.058	
Elastic Deformation	0.00038 V		Normal	1	200 µm/V	0.076	
Hemisphere uncertainty	0.01 µm		Rectangular	1.7321	1	0.006	
Combined Standard Uncertainty						0.595	0.000
Expanded Uncertainty (k=2)						1.191	0.000

3924.5 Conclusions

Following the uncertainty evaluation procedure set out in this paper a rigorous evaluation of an axi-symmetric measurement machine was carried out. Expanded uncertainties were calculated at a 95% confidence level for radial runout radial runout (1.2 µm with a plunger probe or 1.7 µm with a lever probe), axial runout (1.2 µm with a plunger probe or 1.5 µm with a lever probe), and coning (0.44 arc seconds with a plunger probe or 0.60 arc seconds with a lever probe).

In order to illustrate the dominant sources of uncertainty each source is shown as a percentage of the combined uncertainty in Fig. 6 and Fig. 7.

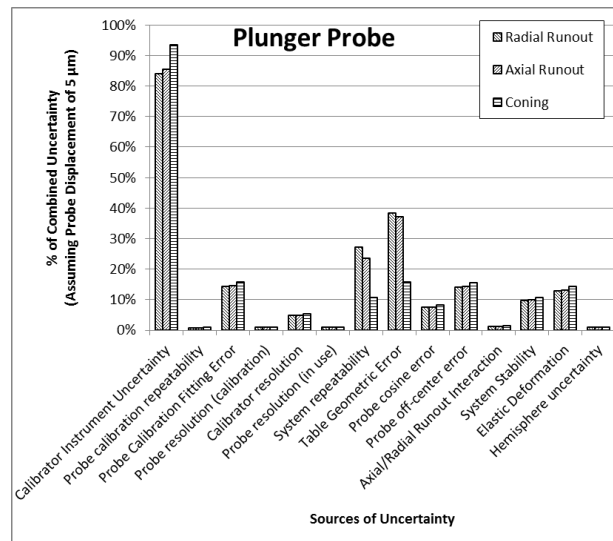


Fig. 6 – Contributions of Uncertainty Sources for Measurements with a Plunger Probe

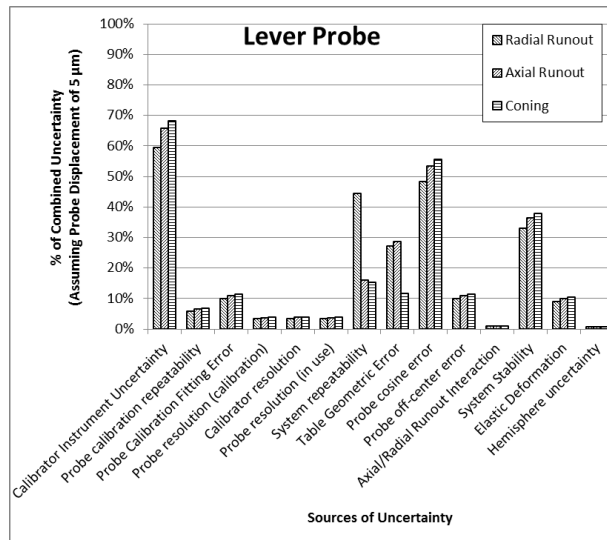


Fig. 7: Contributions of Uncertainty Sources for Measurements with a Lever Probe

When using a plunger probe the uncertainty is dominated by the calibrator uncertainty although the system repeatability and table geometric errors also have some effect for runout measurements. When using a lever probe the calibrator uncertainty remains the most significant and the system repeatability and table geometric errors are also significant. Two probe related sources are also very significant; the probe cosine error and the system stability. The inherent limitations of a lever probe may be difficult to overcome, for high accuracy measurements a plunger probe should therefore be used. If improved accuracy is required then this should be achieved by using an improved calibration process for the probe.

3924.6 Acknowledgements

The research described herein has been carried out as part of the EPSRC, Light Controlled Factory Project (grant No. EP/K018124/1) at the Laboratory for Integrated Metrology Applications (LIMA) in the Mechanical Engineering Department of the University of Bath. Thanks is given to the support and technical expertise from Rotary Precision Instruments, in particular Jim Palmer and Ian Whitehead.

3924.7 References

1. Mei, Z. and P.G. Maropoulos, *Review of the application of flexible, measurement-assisted assembly technology in aircraft manufacturing*. Proceedings of the Institution of Mechanical Engineers, Part B: Journal of Engineering Manufacture, 2014. **228**: p. 1185-1197. DOI: 10.1177/0954405413517387
2. Muelaner, J.E. and P.G. Maropoulos, *Large Volume Metrology Technologies for the Light Controlled Factory*. Procedia CIRP Special Edition for 8th International Conference on Digital Enterprise Technology - DET 2014 – Disruptive Innovation in Manufacturing Engineering towards the 4th Industrial Revolution, 2014. DOI: 10.1016/j.procir.2014.10.026
3. Nielsen, H.S., *Recent developments in International Organization for Standardization geometrical product specification standards and strategic plans for future work*. Proceedings of the Institution of Mechanical Engineers, Part B: Journal of Engineering Manufacture, 2013. **227**: p. 643-649. DOI: 10.1177/0954405412466986
4. UKAS, *M3003 - The Expression of Uncertainty and Confidence in Measurement*. 2007, UKAS, Doc
5. BSI, *General Metrology - Part 3: Guide to the expression of uncertainty in measurement (GUM)*, in *PD 6461-3*. 1995.
6. ISO. *BS EN ISO 14253-2:2011 - Geometrical product specifications (GPS). Inspection by measurement of workpieces and measuring equipment. Guidance for the estimation of uncertainty in GPS measurement, in calibration of measuring equipment and in product verification*. 2011 [cited].